



24th COBEM - 2017



24th ABCM International Congress of Mechanical Engineering  
December 3-8, 2017, Curitiba, PR, Brazil

COBEM2017-2065

## STUDY ON THE DISSIPATION OF KINETIC ENERGY IN IMPACT OF FREE-FALL OBJECTS ON METALLIC PLATES AND ITS ASSOCIATED PLASTIC DEFORMATION

**Camila Marinho Clemente**

**Henrique Gomes Moura**

Faculdade Gama – FGA, Universidade de Brasília – UnB, St. Lestes Projeção A – Gama Leste, Brasília

camila.mcclemente@gmail.com

hgmoura@yahoo.com

**Abstract.** Since the beginning of mass production, vehicle safety has been the focus of constant study and development, especially in recent decades, with the development of materials, manufacturing processes and associated technologies. Particularly as regard heavy vehicles in agriculture, mining and civil construction, the need to increase the safety conditions of operators has forced the protection structures against high impact loads to evolve from nonexistence to the recent view of compulsion. In this paper, it is introduced a theoretical study on the plasticity phenomenon in metals, a computational analysis of the kinetic energy dissipation and the plastic deformation of metallic plates under high impacts, in order to simulate the conditions of the use of a FOPS (Falling Object Protection System) structure, and an experimental analysis of the deformation and energy behavior of the impact of a body on a metal sheet (drop-test), considering the established in standards. This paper was carried out for the elaboration of an Undergraduate Thesis. Thus, this article represents a reduced version of the complete work, which can be consulted in the online repository of the University of Brasília.

**Keywords:** *FOPS, Impact Tests, Plasticity*

### 1. INTRODUCTION

#### 1.1 Contextualização

From the popularization of the automobile in the first half of the twentieth century, the concern with vehicle safety became the target of research and development, causing a noticeable evolution in our available safety parameters. The creation of specific legislation, international standards, crash test models, consumer tests and comparisons between safety tests have resulted in generations of increasingly safe automobiles (CHRISTENSEN & BASTIEN, 2016).

One of the main causes of the evolution of vehicle safety was the advance in the field of engineering. The tools developed, especially the computational tools, as well as the knowledge acquired by constant research and technology, have not only brought about advances in the optimization of automotive systems - as they relate to the geometry of structures, their materials and manufacturing processes - but also better management of the decelerations and the applied forces on the occupants (CHRISTENSEN & BASTIEN, 2016). Of note among these engineering advances are the already mentioned computational tools and the studies related to the plastic behavior of the materials. Both allowed to predict how the loads, static and dynamic, applied to a structure would deform it, guaranteeing to the designer the previous knowledge if the system on a given load would absorb it adequately (not allowing the deformations to invade the volume limit of deflection and to reach the occupants) or not.

This vehicle safety revolution (CHRISTENSEN & BASTIEN, 2016) has also reached sectors of the automotive industry that are away from the popular consumer. In the production and service sectors, such as agriculture and mining, the development and application of protective structures against accidents common to areas such as Roll-Over Protection Structure (ROPS), and FOPS (Falling Over Protection Structure), Fig. (1), against falling objects, has proved essential in the quest to ensure the safety of machine operators such as tractors and excavators. Studies show that the use of ROPS and equivalent structures reduced to zero the number of fatalities due to overturning of tractors in North-European countries (REYNOLDS & GROVES, 2008).



Figure 1. Agricultural vehicle with FOPS. Source: JOHN DEERE SALES MANUAL, 2013

## 1.2 Elasticity and Plasticity

For an efficient analysis of the deformations related to the impact of loads on sheets, it is necessary a study on the deformation modes of a material under tension, highlighting here the behavior of the materials in the so-called elastic and plastic regimes. It is also convenient to analyze dynamic loads of impact type and how the material of a structure behaves when subjected to them.

As for the behavior of the material, the deformation is presented in a varied way according to the observed regime. In the so-called elastic regime, once the load causing the deformation is suspended, it is reversible (ASKELAND & PHULÉ, 2006), not affecting the geometric characteristics (dimensions) of the bodies under tension permanently. When we observe stresses that cause only elastic deformations, "elastic regime", it focuses on the linear part of the strain-strain graph, shown in Fig. (2). In this regime, the deformation of the material is proportional to the applied stress, respecting Hooke's Law, which establishes  $\sigma = E\varepsilon$ , where  $\sigma$  corresponds to the applied stress, E to the Young's Modulus of the material and  $\varepsilon$  to the deformation (ASKELAND & PHULÉ, 2006; CALLISTER, 2007).

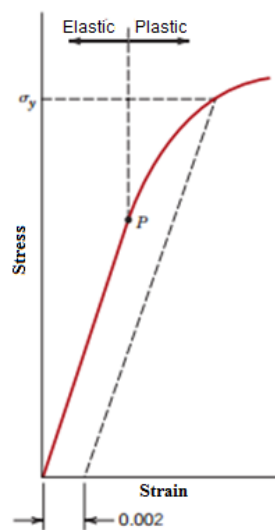


Figure 2. Generalized stress-strain curve. The line parallel to the linear part of the graph, when touching the curve determines the limit of hardening of the material. Source: [CALLISTER, 2007.](#)

The Young's Modulus is the slope of the line in the stress-strain curve (ASKELAND & PHULÉ, 2006; CALLISTER, 2007). This parameter is considered a measure of the stiffness of a material (ASKELAND & PHULÉ, 2006), and can be seen as a measure of the material's resistance to deformation (CALLISTER, 2007). The greater the Young's modulus, the greater the atomic bonding forces and the greater the required stress, or the energy applied, to separate the atoms, causing the elastic deformation (ASKELAND & PHULÉ, 2006). The Young's Modulus of a material is obtained by the tensile test, which generates the stress-strain curve. In the graph, this value corresponds to that of the stress at the point where the curve passes from the linear (elastic) to non-linear (plastic) regime.

The deformation that occurs in the plastic regime of the material is the one that is permanent, which begins after the elastic and linear step of the deformation, when its rate is not more proportional to the applied stress. (ASKELAND & PHULÉ, 2006; CALLISTER, 2007). For this phase, therefore, Hooke's Law no longer describes the behavior of the material under load, the deformation occurs at the crystalline level and the displacement of the atoms remains after the withdrawal of the charge (LEMAITRE & CHABOCHE, 1994). Unlike the elastic deformation, in which the interatomic

bonds are only elongated, the plastic deformation causes the rupture and reconstruction of these bonds, in addition to the movement of the lattice planes (Dunne & Petrinic, 2005).

A fundamental parameter for the study of plasticity is the Yield Limit of the material, which corresponds to the stress value related to the point of encounter between the curve of the stress-strain graph and the line parallel to the linear part thereof, drawn from the 0.002 point in the abscissa axis (0.2% deformation). This limit demarcates the point from which the material is plastically deformed, and it is from this that it is possible to analyze which tensions generate what types of deformations, separating those responsible for the elastic of the plastic (LODI, 1998) .

The yield limit is dependent on the rate of deformation applied to the structure (Jorge & Dinis, 2004/2005). The change in the yield limit of a material is related to the hardening law, which defines the conditions for a new yield to occur as the load is applied and the material is hardened. In so-called Isotropic Hardening, the surface runoff of the material is variable as stress is applied to it, which defines a hardening parameter other than zero, causing a change in the hardness of the material under loading and followed by hardening points, in addition to a variation in the yield stress (SANDOVAL, 2014). This type of hardening is observed in the study of falling objects on metal sheets at ambient temperatures.

Another factor influencing plasticity is the hardening, which corresponds to the elevation of the resistance of a material by the deformation. This phenomenon is caused when an applied load causes in the material an increase of the disagreements, causing a greater difficulty of mobility between the atoms of the material. Thus, higher stresses will be required to cause sliding of atoms and planes and, consequently, deformations (ASKELAND & PHULÉ, 2006). As the application of a load causes constant surface changes in the material, the amount of dislocations at the microstructural level is increasing while subjecting the structure to loading, which causes a constant increase of hardness, that is, the difficulty in deforming the material, something modulated by the Hardening Law.

However, in order to analyze the plastic aspects of a stress-strain system, it is first necessary to observe the behavior of the system in question. Each behavior is defined by a constitutive model, which describes how the deformations inherent to the load-structure assembly are given and evaluated. The model suitable for the study in question is the elasto-plastic, which covers the elastic and plastic behavior of the materials (SANDOVAL, 2014). Some properties inherent to this model are the existence of an elastic domain, delimited by a yield function, the occurrence of permanent deformation, which respects the flow rule, considering the type of loading applied, and the surface hardening with its consequent modifications of mechanical properties (POCKSZEWNICKI, 2004).

### 1.3 Objective

The objective of this work is the computational simulation of a system of falling objects on metallic plates, such as those used in FOPS (Falling Over Protection System) automotive protective structures, according to the defined guidelines by the standards NBR NM-ISO 3164, NBR ISO 9248, NBR ISO 9248 and NBR NM-ISO 3449, the construction of an impact test apparatus on sheet and the realization of the related experiment observing ISO 3449.

## 2. METHOD AND MATERIALS

A computational simulation was performed to observe the behavior of a laterally set metal sheet when struck by an impact rigid body. The results obtained allowed the development of an experimental apparatus for the real reproduction of a condition analogous to the simulated one, observing the associated energy levels. The experimental strategy consisted in raising the impact body at a given time, so that the potential energy stored by it was equivalent to the desired mechanical system. Once the calculated height was reached, the body was released in free fall, reaching the center of the metal plate, positioned attached to a metal table underneath the impact body. During the fall, the gravitational potential energy ( $E_{pg}$ ) is gradually transformed into kinetic energy ( $E_c$ ) and, upon reaching the plate, in plastic energy (internal, absorbed by the plate in deformation) and elastic (kinetic) energy.

To aid in the development of the prototype and the analysis of the results, a computational simulation was established as part of the experimental strategy. The computational analysis, performed on a simplified and approximate real system, aimed to present preliminary results on the behavior of the test piece after the shock, besides allowing a discussion about the reaction of the impacted plate in relation to the raised theory. However, the experimental study focuses on observing the actual deformation on the sheet metal after impact, comparing it with that obtained in the preliminary analyzes, as well as the energy behavior of the system, especially the mechanical energy (initially in the gravitational potential form) absorbed by the body of evidence.

### 2.1 Computational Simulation

#### 2.1.1 Method

For computational analysis, we observed the geometry of the test bodies and the parameters that define the conditions of the analysis. Once these characteristics were raised, the simulation was performed according to the following:

- CAD model of the structure (plate and impact cylinder) in CATIA v5 software;
- Import of the geometry to Explicit Dynamics of the Ansys software (analysis by MEF);

- Choice of material in the Ansys library and configuration of mechanical properties;
- Assignment of the material to the imported geometry;
- Choice of element size and mesh generation;
- Input of analysis parameters;
- Simulation starts;
- Collection and analysis of results

### 2.1.2 Materials

For the computational analysis, two steel plates, of 1 x 1 x 0.003 m and 1 x 1 x 0.001 m, and two impact bodies (Fig. 3) were molded according to the specifications established in ISO 3449. The material assigned to the system was Steel Structural.

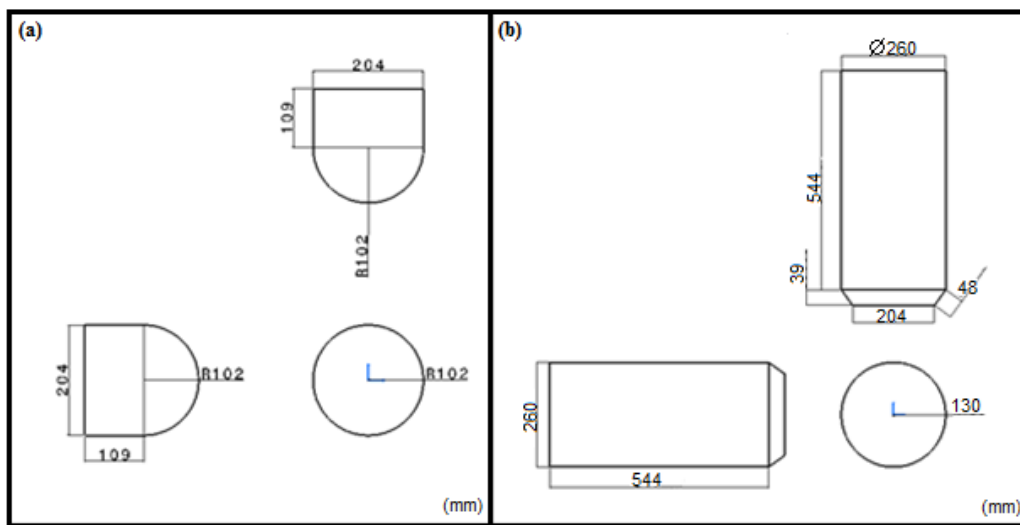


Figure 3. Dimensions of impact bodies (ISO 3449) for level I (a) and level II (b) tests.

### 2.1.3 Entry Parameters

For the simulation of the system of falling objects, and the associated impact, it was observed that the platform Explicit Dynamics, integral of the interface of Ansys, was the most indicated. The software manual itself (ANSYS Explicit Dynamics Brochure, 2011) indicates the tool for so-called Drop Tests and also those involving material failure, which corresponds to plastic deformations. The input parameters used are listed in Tab. 1.

Table 1. Parameters used in the simulations.

Parameter	Value	Parameter	Value
<b>Coefficient of friction</b>	0,57	<b>Mass (impact body - level I)</b>	45 kg
<b>Time of analysis (end time)</b>	0,02 s	<b>Mass (impact body - level II)</b>	227 kg
<b>Energy (level I)</b>	1365 J	<b>Impact velocity (level I)</b>	7,79 m/s
<b>Energy (level II)</b>	11600 J	<b>Impact velocity (level II)</b>	10,1 m/s

As for the supports, the board was assigned fixed supports, since in its real system this would be embedded. The sheet was set two of its sides, both parallel to each other.

### 2.2 Experimental Procedure

The experimental test consisted in raising the impact body at a given height so that it accumulated associated potential energy equivalent to that referred to in the standard and releasing it in free fall on a metal plate set on a fixing structure, deforming it in impact. The data collected were the deformations, in millimeters, of the plates tested, the accelerations of the system and the sound of the impact between the impact body and the test body.

### 2.2.1 Method

For the test, a lifting structure was assembled which consisted of a system of pulleys and ropes associated with a pair of electromagnets. Once an electric current was supplied to the magnetic assembly, it was attached to the impact body, allowing its elevation. Upon reaching the stipulated height, calculated at 2,923 m, the current was cut off, extinguishing the magnetism and releasing the impact body on the metal plate, which was screwed onto the fixed structure and positioned so that its geometric center coincided with of the impact body. Figure 4 shows the assembled system.



Figure 4. Impact body on fixation plate-structure assembly; it is observed the support of the impact body by electromagnets coupled to the pulley system and the plate.

The instrumentation of the system was made before the impact body was raised. The projectile was constructed so as to allow its central opening, allowing the accelerometer to fit close to its center of gravity.

### 2.2.2. Materials

- 1 impact body (Fig. 5), in geometry and dimensions determined by ISO 3449, divided into two parts, threaded together and made of ASTM1045 steel. Total body mass: 47.65 kg.

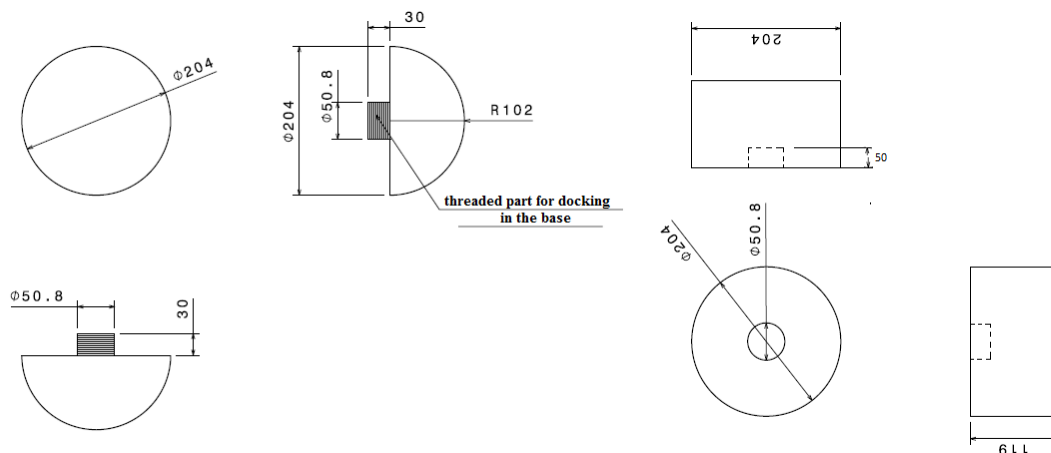


Figure 5. Geometry and dimensions (mm) of the two parts that together form the impact body.

- 2 500x500x0.9 mm plates in ASTM 1020 steel
- 2 electromagnets and 2 5A sources.
- 8 steel screws and 16mm diameter
- 1 fixing table, 1 rope and 2 pulleys
- 1 MPU6050 accelerometer
- Cable, caliper and cables for connection of the electromagnet and electronic connections

### 2.2.3. Measuring System

For the measurements of the experimental data, two systems are used: one dedicated to the measurement of plastic deformation and another to the associated energies. In the first one, the systems used were those associated with measurements of geometric dimensions. They include, therefore, a measuring tape, ruler and caliper. Deformations in the order of centimeters allowed such instruments to be adequate.

In relation to the associated energies, a measurement strategy was elaborated with greater apparatus and caution, since the object of measurement, energy, is not material. In this way, it was decided to use indirect measurement techniques, associated with sound recordings, to detect the moments of the impacts against the plate, and to accelerometers (MPU 6050, connected to an Arduino UNO3 and a Laptop) positioned in the center of mass of the impact body, Fig. 6, to obtain the energy of the system.

The sound recordings provided the time intervals between the impact first (shock against the plate after the free fall) and the second (bounce after the first shock), allowing to calculate, approximately, the height reached by the bounce and the energy that made possible the ascent under the conditions in which they occurred.



Figure 6. Accelerometer in the center of the impact body and coupled impact body.

## 3. RESULTS AND DISCUSSION

### 3.1 Computational Simulation

The results obtained by the analysis point to the plastic deformation of the plate and the behavior of the mechanical energy of the system, divided into kinetic energy, internal energy, hourglass energy and contact energy. Tables 2, 3 and 4 point out the results of the simulations for different element sizes and energy levels associated with impacts.

Table 2. Results for impact on 3 mm thick sheet and 1365 J absorbed

Element Size (m)	0,02	0,0175	0,015	0,0125	0,01
Number of Cycles	79620	45710	55640	75884	98530
Increased Time (s)	2.445E-07s	4.376E-07s	3.594E-07s	2.636E-07	2.030E-07
Total Energy (J)	1362,3	1365,1	1367,4	1369,6	1371,5
Kinetic Initial Energy (J)	1362,3	1365,1	1367,4	1369,6	1371,5
Kinetic Final Energy (J)	258,4	269	260,3	260,3	260,3
Intern Initial Energy (J)	-	-	-	-	-
Intern Final Energy (J)	1101,6	1101,6	1109,7	1097,15	1097,15
Elastic Energy (J)	258,4	269	260,3	260,3	260,3
Plastic Energy (J)	1101,6	1101,6	1109,7	1097,15	1097,15
Hourglass Energy	244,8	231,2	164,4	164,4	164,4
Contact Energy (J)	-	-	-	-	-
Maximum Plastic Deformation – Sheet (m)	0,070151	0,074091	0,073088	0,071115	0,069802
Maximum Plastic Deformation – Cylinder (m)	0,00	0,00	0,00	0,00	0,00

Table 3. Results for impact on 3 mm thick sheet and 11600 J absorbed

<b>Element Size (m)</b>	<b>0,025</b>	<b>0,02</b>	<b>0,015</b>	<b>0,0125</b>	<b>0,01</b>
<b>Number of Cycles</b>	104299	375427	128875	136892	128437
<b>Increased Time (s)</b>	1.920E-07s	5.306E-08s	1.552E-07s	1.463E-07	1.553E-07s
<b>Total Energy (J)</b>	12159	12193	12216	12225	12234
<b>Kinetic Initial Energy (J)</b>	12159	12193	12216	12225	12234
<b>Kinetic Final Energy (J)</b>	511,4	542,03	554,53	551,5	551
<b>Intern Initial Energy (J)</b>	-	-	-	-	-
<b>Intern Final Energy (J)</b>	11560	11636	11670	11674,5	11683,5
<b>Elastic Energy (J)</b>	511,4	542,03	554,53	551,5	551
<b>Plastic Energy (J)</b>	11560	11636	11670	11674,5	11686,5
<b>Hourglass Energy</b>	615	677	693,16	689,38	688,77
<b>Contact Energy (J)</b>	-	-	-	-	-
<b>Maximum Plastic Deformation – Sheet (m)</b>	0,07627	0,088939	0,10819	0,12225	0,13604
<b>Maximum Plastic Deformation – Cylinder (m)</b>	0,00	0,00	0,00	0,00	0,00

Table 4. Results for impact on sheet of 1 mm thickness and 1365 J absorbed

<b>Element Size (m)</b>	<b>0,01</b>
<b>Number of Cycles</b>	162994
<b>Increased Time (s)</b>	1.178E-07
<b>Total Energy (J)</b>	1371,5
<b>Kinetic Initial Energy (J)</b>	1371,5
<b>Kinetic Final Energy (J)</b>	114,5
<b>Intern Initial Energy (J)</b>	-
<b>Intern Final Energy (J)</b>	1507
<b>Elastic Energy (J)</b>	114,5
<b>Plastic Energy (J)</b>	1507
<b>Hourglass Energy</b>	78,5
<b>Contact Energy (J)</b>	-
<b>Maximum Plastic Deformation – Sheet (m)</b>	0,10032
<b>Maximum Plastic Deformation – Cylinder (m)</b>	0,00

The permanent deformations of the sheet shows the plastic aspect of the deformations (LEMAITRE & CHABOCHE, 1994; DUNNE & PETRINIC, 2005), once the withdrawal of the load didn't cause the sheet to restore its first form. However, the energetic recovery that the system shows, which allows the impact body to return to its previous movement in an approximated direction (free fall), but opposite orientation – in a movement of bounce, indicates that there is elastic energy associated to the phenomenon, in a Elastic-Plastic system.

The energy related to the elastic deformation corresponds to the final kinetic energy, observed both in the computational simulation and in the experimental tests. In the first one, the energy values varied according to the discretized mesh, but their differences between them were relatively small, in the order of 0.77% the largest of them (energy level I). Still on the energy, in the simulation, the conservation of the mechanical energy and the transformation behavior of this one, from kinetic to internal (plastic), is observed, which respected the expected in all the simulations. On the other hand, the energy called Hourglass, related to the mesh distortion (LSTC, 2010) (which occurred in the impact body, not in the plate), maintained acceptable values between 5% and 17%. It is emphasized that, because it is not related to the plate, it is not expected that this will compromise the obtained values of deformation.

In relation to the deformation, this was limited to the plate, is permanent (plastic) and is, as expected, linked to the hardening of the material, caused by the hardening of the after impact, since in a dynamic load condition, it is possible to see permanent deformation under tensions lower than expected for each material. It has also been observed that the hardening of the material was of the isotropic type, i.e., the yield is variable as tension is applied thereto (SANDOVAL, 2014).

The positioning of the FOPS should observe the maximum deformations shown. The plastic deformations presented by the tests with the requirements required to Level I and 3mm thick plate did not exceed 9 mm of deformation. Thus, the FOPS should be positioned so that it is above the DVL by at least 9 mm, without considering a safety factor. In relation

to Level II, although the values of the deformations in the center of the plate were not high, those of the edges were out of order and elevated. Therefore, if you wish to use the 3mm plate for a FOPS capable of meeting the requirement of 11600 J, design adjustments must be made, such as a change in the settings or position of the plate in relation to the DVL, to ensure that this is not invaded by the deformed plate.

### 3.2 Experimental Procedure

The objects of measurement of the experiment were the plastic deformations in the plate and the energies associated to the system. Two tests were carried out, both following the same mounting system already described in the method in this section.

#### 3.2.1 Deformations

Table 5. Lateral deformations of plates 1 and 2

	Initial Dimensions (mm)				Final Dimensions (mm)				
	Side A	Side B	Side C	Side D	Side A	Side B	Side C	Side D	Depth
<b>Sheet 1</b>	500	501	499	500	489	497	456	471	881
<b>Sheet 2</b>	500	501	501	500	474	464	456	492	868

It was observed, as in the computational simulation, that the elastic-plastic model is the one that best defines the system tested, since in this there are permanent (plastic) and non-permanent (elastic) deformations, which are evidenced by the bounce of the impact body, that is, in its upward movement after impact on the plate, which describes a direction trajectory equal to the free fall, but opposite orientation. It is also valid to point out that such upward movement is a consequence of the transformation of the elastic energy (related to the deformations of this type) into kinetic energy. However, the deformation form, observed in the sinking of the plate, was not symmetrical as expected, and would be explained by the isometry of the material. The slight inclination of the impact body during the fall, which caused an impact whose vertical axis of the projectile did not coincide with the center of the plate, as in the simulation, resulted in a shock that deformed the plate non-symmetrically. In addition, there was the second impact of the body on the plate, caused by the bounce of the first one, which also generated a ray of experimental deformation larger than the simulated one. Nevertheless, it is worth mentioning that the experimental radius was considerably larger than the computational radius, which leads us to believe that other factors, as yet unidentified, influenced its size. Figures 7, 8 and 9 show the deformed plates.

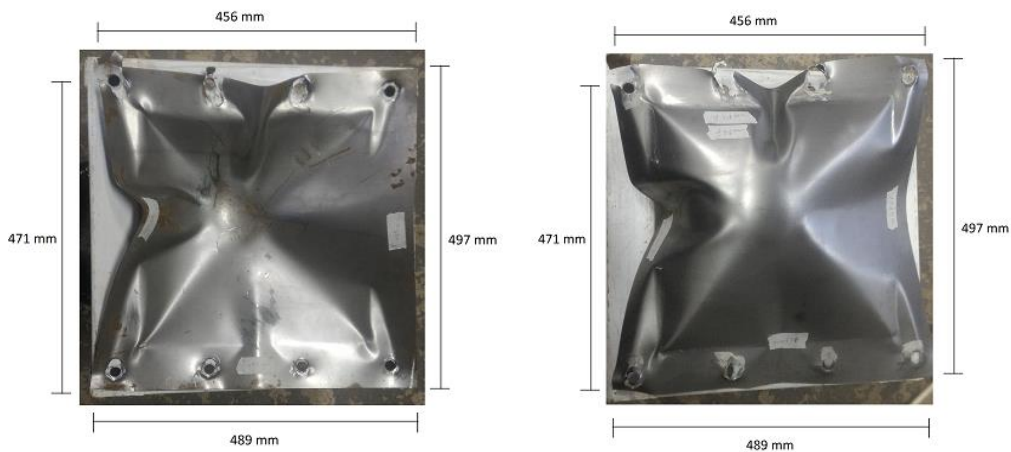


Figure 7. Plate 1 after impact (top and bottom view)

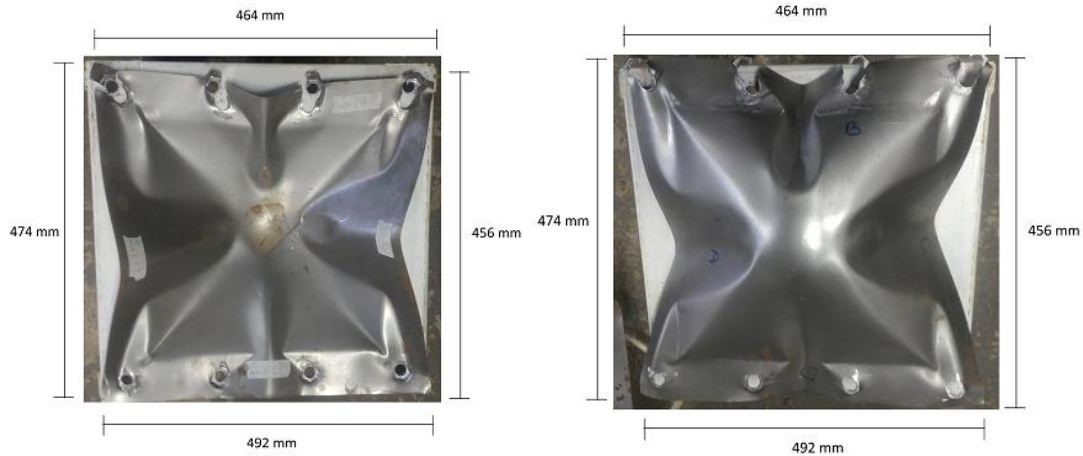


Figure 8. Plate 2 after impact (top and bottom view)



Figure 9. Plate 1 (left) and 2 (right) after impact (bottom view)

### 3.2.2 Accelerations and Forces

Initially, it was decided to use an accelerometer, positioned near the center of mass of the impact body, to measure the accelerations associated with fall and impact. However, the very high accelerations caused the saturation of the sensor, which was not able to measure the values related to the impact of the projectile on the plate. Another approach, then, was triggered,

Using the recorded videos of the trials, in slow motion by the iPhone 5s smartphone, the audio was extracted by the software Audacity, obtaining the associated sound wave. Observing its peaks, it was possible to determine the time interval between the first impact (caused by the free fall of the body to the plate) and the second (related to the bounce). This interval, of approximately 1.125s, for calculation purposes, should be divided by four, since the recording occurred in slow motion (in an order of  $\frac{1}{4}$  of a second per second). It is also worth noting that the interval indicates the time of rise and fall. Approaching the movement of the body to a parabola, we have that the time of fall is equal to that of rise and that gravity corresponds to the acceleration the fall. Thus, Equation 1 indicates the calculations made to estimate the height that the projectile acquired after the first impact. Given the height, and considering an energy loss of one-third, it is estimated that the kinetic energy supplied by the plate to the body (by means of elastic energy) was 29.89 J. This being the kinetic energy, the absorbed plastic energy added to the energy dissipated (in sound and thermal energy, for example) is 1372 J - the initial energy of 1402J is considered, as shown in Eq. 2.

$$\Delta S = V_0 t + \frac{at^2}{2} \quad (1)$$

$$\Delta S = \frac{9,808 \times \left(\frac{1,125}{8}\right)^2}{2}$$

$$\Delta S = 0,09697 \text{ m}$$

$$E_{pg} = mgh = 47,65 \times 9,808 \times 3 = 1,402 \text{ J} \quad (2)$$

The energy values, therefore, differ from those obtained in the simulations, which corresponded to 107 J for elastic and 1279 J for plastic. The reasons for the difference are given by the isolated character of the simulation, which does not consider losses, and by the assembly of the experiment, which differs from the simulated model, since adaptations were necessary for the test. The plate is set in full dimension on two sides in the simulation, and not screwed as done in the experiment. The coupling in the simulation was necessary to reduce the computational cost, since the model with screws and different contact conditions increased the interactions and contour conditions of the model. In addition, the shock occurs exactly at the center of the plate in the simulation, while in the test it occurred with the impact body slightly inclined, affecting the symmetrical deformations and the conversion of elastic energy in the plate in kinetic on the specimen.

#### 4. CONCLUSION

The objective of this work was the construction of a bench for impact tests against sheet metal, observing the orientations pointed out by ISSO 3449. For this, computational simulations of a simplified model were carried out, which guided the definition of the characteristics of the bench, and provided information on plate deformations and energy behavior. Computationally, the plastic deformation characteristic of impact situations and the transformation of kinetic energy into plastic (or internal, as named by the software) were observed.

As for the construction of the bench, this considered the structure of elevation of the impact body, the structure of fixation of the plate and the instrumentation of the system. The body was raised to such a height, in order to store, by means of gravitational potential energy, the energy values required in the standard. The elevation was made by a system of rope, pulleys and electromagnets. The fixing of the sheet to a rigid metal frame was carried out by means of screws with dimensions calculated to avoid deformation. Already the instrumentation was divided between the one related to the geometric measurements and the one responsible for the data that allowed the calculation of energy (audio recording and accelerometer). Due to the high values of acceleration, the sensor responsible for this saturated and its data were disregarded. Thus, the energies of the system were calculated by means of the recorded recordings.

The data obtained experimentally do not match those provided by the computational analyzes. Although the deformations are not very different, the energies point values far from each other. This is due to the non-perfect isolation of the experimental system, as occurs in the computational (since the system was simplified due to the computational cost). Thus, it is concluded that the computational model is not the most appropriate to the real conditions, but the efficiency of the experimental bench in the operation and the data of plastic deformation and energy conversion is emphasized.

#### 5. REFERENCES

- ANSYS, Explicit Dynamics Brochure, 2011.
- ASKELAND, D. R.; PHULÉ, P. P. *Ciência e Engenharia dos Materiais*. Estados Unidos: CENGAGE Learning, 2008.
- CALLISTER, W. D. Jr. *Materials Science and Engineering: an Introduction*. Estados Unidos: John Willey & Sons, 2007.
- CHRISTENSEN, J.; BASTIEN, C. *Nonlinear optimization of vehicle safety structures: Modeling of structures subjected to large deformations*. Oxford: Elsevier, 2016.
- DUNNE, F.; PETRINICK, N. *Introduction to Computational Plasticity*. Oxford: Oxford University Press: 2005.
- JORGE, R. M. N.; DINIS, L. M. J. S. *Teoria da Plasticidade*. Departamento de Engenharia da Universidade do Porto. Porto, 2004/2005.
- LEMAITRE, J.; CHABOCHE, J. L. *Mechanics of Solid Materials*. Cambridge: Cambridge University Press: 1994.
- LODI, P. C. *Aplicação do Modelo Clam-clay modificado a um solo arenoso*. 1998. 144f. Tese (Mestrado em Geotecnia) – Escola de Engenharia de São Carlos, Universidade de São Paulo, São Paulo, 1998.
- REYNOLDS, J. S.; GROVES W. Effectiveness of roll-over protective structures in reducing farm tractor fatalities. *American Journal of Preventive Medicine*. v. 18, n. 4S. p.63-69, 2000.
- SANDOVAL, C. F. B. *Modelos elasto-plástico e sua influência no processo de dimensionamento de componentes mecânicos*. 2014. 111f. Tese (Mestrado em Ciências Mecânicas). Departamento de Engenharia Mecânica, Universidade de Brasília, Brasília, 2014.

#### 6. RESPONSIBILITY NOTICE

The authors are the only responsible for the printed material included in this paper.